An Investigation of Methanol and Methanol Blended Sprays Using Laser Scattering Images

Wook Choi
Chonnam National University, Dept. of Mechanical Engineering 300 Yongbongdong Buk-Gu, Gwangju, 500-757, Korea
Byung-Chul Choi*
Chonnam National University, Dept. of Mechanical Engineering 300 Yongbongdong Buk-Gu, Gwangju, 500-757, Korea

The characteristics of methanol and methanol blended (M85) sprays were investigated under atmospheric conditions at various temperatures, ranging from non-vaporizing to vaporizing ambient conditions (298~353 K). From laser scattering images, the macroscopic characteristics of the spray, such as the spray tip penetration and the spray angle, were determined. Entropy concept was introduced to represent homogeneity and PIV analysis was adopted to determine the fluid dynamic information at each location of the spray. The correlation between entropy and vorticity strength enabled us to find their relations. The effect of ambient composition, mainly of viscous effect as affected by CO_2 levels, was investigated using PIV and entropy analysis. Spray width and entropy value were found to tend to decrease at increased CO_2 levels.

Key Words: Spray, Methanol, Spray Tip Penetration, Spray Angle, Entropy Analysis, PIV, Vorticity

1. Introduction

Methanol, is receiving attention as one of the future alternative fuels and is already commercialized in some countries, but has rather inferior spray atomization characteristics as compared to gasoline because of its somewhat higher viscosity and lower vapor pressure even under room temperature (Suga et al., 1990), let alone under cold ambient condition. So, it is vital to promote atomization by adopting extra injection systems or schemes. There are some examples of remedies for the problem, such as an ultrasonic injector (Kazuyoshi et al., 1989) or the utilization of the flash boiling effect by heating fuel near to its boiling point at low ambient pressure (Kim et al., 1980). In addition, additives or intake air heating also can be addressed as solutions. Adding gasoline to improve the volatility or heating intake air, particularly, by EGR (Exhaust Gas Recirculation) can be recommended as the more easily applicable solutions in spite of some practical limitations (Lee et al., 1992). By applying these methods to promote evaporation, enhancement of spray dispersion under ambient conditions becomes possible, and of course, preventing 'wall wetting' due to liquid film formation.

Methanol, as a pure compound, has low boiling point (338 K) so that it is possible to utilize its vaporization characteristics under normal operating conditions. Spray characteristics can be greatly changed under the vaporizing environment compared with the non-vaporizing condition. Once vaporization has started, dispersion to the ambient is promoted so that mixedness of spray can be improved. The mixing

* Corresponding Author,
E-mail : bcchoi@chonnam.ac.kr
TEL : +82-62-530-1681; **FAX** : +82-62-530-1681
Chonnam National University, Dept. of Mechanical Engineering 300 Yongbongdong Buk-Gu, Gwangju, 500-757, Korea. (Manuscript **Received** May 8, 2001; **Revised** September 21, 2001)

mechanism, mainly occurs by momentum exchange due to viscous friction, and can be altered to a direct diffusion mechanism under vaporizing conditions. So it is necessary to understand in depth the characteristics of sprays in such conditions.

The mixing and diffusion of spray are important factors in the formation of a homogeneous mixture. However, there seems to be no easy way to describe them (Lee et al., 1999). It is even difficult to tell how large the volume of interest or how long the time should be when defining the degree of mixing, or perhaps homogeneity. So, the statistical entropy concept was adopted to represent the homogeneity of mixing or diffusion process for confined small areas on the spray boundary. The reason why the terms between mixing and diffusion are differentiated is that the physical phenomena occurring on the spray boundaries are different, principally "mixing" or "macro mixing" applies to the non-vaporizing condition, and is unlike molecular "diffusion" more applicable in the case of vaporization. In a vaporizing environment, the use of term "diffusion" or "part diffusion" at the molecular level may be more accurate. In describing the characteristics for ambient conditions, entropy concept would be very useful. Using entropy as a concept, the potential for a homogeneous mixture field to be formed can be inferred by watching the initial mixture formation process.

In the present study, the spray characteristics of methanol and methanol blended (M85: methanol 85, gasoline 15 by vol. %) were investigated by introducing the entropy concept, which represents the homogeneity, calculated from laser scattering images. Velocity and vorticity distributions were obtained by PIV (Particle Image Velocimetry), the correlation between entropy and vorticity strength and the effect of ambient composition are also discussed.

2. Experimental Apparatus and Procedure

Figure 1 is a schematic diagram of the experimental apparatus used in this work. It

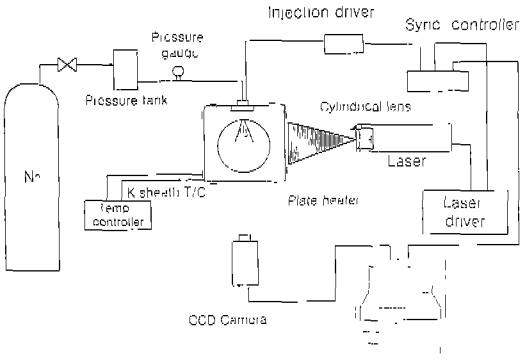

Fig. 1 Schematic diagram of experimental apparatus

consists of a constant volume combustion chamber (CVCC) used as an injection chamber, an injection system, an image acquisition system and a laser.

The CVCC has three quartz windows, of 120 mm(ϕ) $\times$25 mm(t), for visualizing, at the front and the sides. Five plate heaters of 100 W were placed on the upper, lower, left, right and front side for heating the chamber. Thermocouples (K-sheath) and temperature controllers were used for measuring and controlling temperatures. Though it might be believed that a homogeneous temperature field could be formed by heating for a long time, the real temperature field was ascertained by constructing a plastic window. The window had 57 holes to allow sequential thermocouple insertion to measure temperatures under steady-state conditions. From these measurements, temperatures could be determined on a spatial basis. The standard deviation of the temperature field was within $\pm$3 K. The representative temperature was based on the average of measured values. Ambient temperature conditions were set to 298 K, 323 K, 338 K and 353 K, after considering preheating effect by the EGR. Particularly, since 338 K is the boiling point of methanol, dramatic changes are detected around this point.

In case of measuring the spray changes under ambient composition, CO_2 was charged from 5 to 25 % after reducing the pressure inside the chamber with a vacuum pump. Ambient pressure was set to 1 bar for all tests.

Table 1 Experimental conditions

Injection system	Nitrogen gas driven accumulator type
Injector type	Solenoid driven pintle type
Hole diameter(mm)	0.3
Injection duration(ms)	3.0
Fuel	Methanol, M85
Injection pressure(bar)	3(gauge)
Ambient temperature(K)	293, 323, 338, 353
Ambient pressure(bar)	1.0
Ambient gas composition	Air(100%), Air(95%)+CO_2(5%), Air(90%)+CO_2(10%) Air(75%)+CO_2(25%) (vol.%)

The injector used was a pintle type of gasoline injector and the effective injection pressure was 3 bar. The reason why we selected the pintle type was that it is commonly used and showed apparent spray angles even at low injection pressure. The fuel pressurized by nitrogen was injected with a controlling circuit and injection duration was set to 3 ms. The fuels of interest were methanol and M85.

Above-mentioned experimental conditions are summarized in Table 1.

For capturing images, the cross-correlation CCD camera (Pulnix 9701, Dual) with 105 mm lens (Nikon, macro Nikorr) and the image grabber (OFS323, Dual) were used. Captured images were stored and processed later on a computer.

The laser used was a semi-conductor pulse laser (Oxford, 805 nm, 25 mJ/p). Though the pulse duration was rather wide, of the order of 1 microsecond at minimum, no blurring was seen, and proved to be both very useful and easy to control for this low speed spray measurement.

The optical arrangements for capturing images were same for all tests, because the entropy analysis and the PIV analysis were made on identical scattering images. In other words, the angle between the laser and the camera was 90° and the laser sheet made using a cylindrical lens was collimated to the center of spray. The interval between laser pulses was 100 μs and the laser

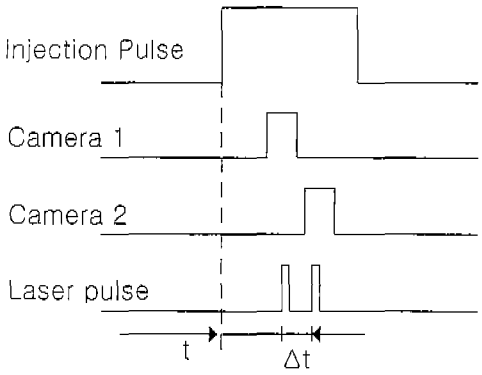

Fig. 2 Timing diagram for image acquisition

pulses were synchronized with each exposure time of the cross-correlation camera.

The pulse diagram is shown on Fig. 2. The cross-correlation algorithm was used for deriving velocity vectors, and the software used for this work was VidPIV (Ver. 4.0, Optical Flow System).

To apply the entropy and PIV analysis to the same area, 4 interrogation areas (64 pixels×64 pixels, respectively) were set on different positions in each spray image. The interrogation regions were placed on the relative locations to the reference ones in Fig. 3, considering the variation of spray shapes to the different ambient conditions. But the size of each interrogation area was held constant because the entropy value is very sensitive to the mesh size (Yuyama et al., 2000). These areas all contained the boundaries between the spray and the ambient so that the effect of viscous friction could be determined.

In the entropy analysis and the PIV analysis based on a laser scattering image, a strict decision and a coherent application of threshold value are very important.

Some unwanted background noises often not only lead to inexplicable results, but also may affect the analyses adopted in a current study because the experimental results are only dependent on the scattered levels of images. Thus, to minimize the possible interference of unwanted noises, the background scattering levels should be precluded. For this aim, the background image was captured for every imaging, prior to the main

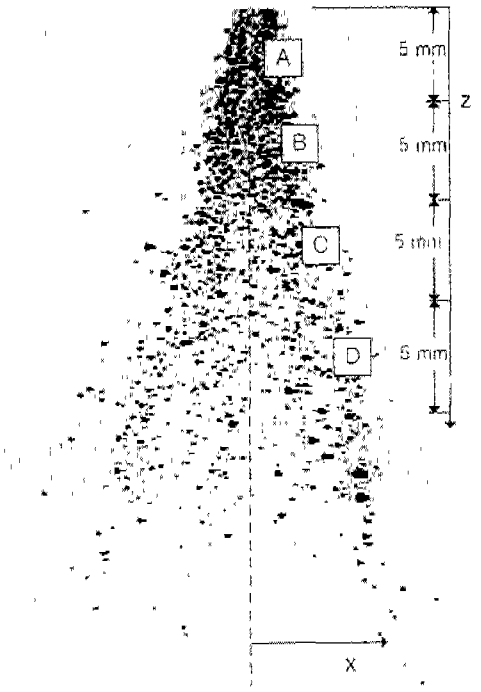

Fig. 3 Typical spray image for analysis

operation. By doing so, the pure image could be derived by subtracting the background levels from the main image. However, possibly due to the variation among each experiment, there were several spots of negative intensity levels in the pure image after the subtraction of background levels, which meant the base intensity level was somewhat unstable. In addition, some small fuel droplets that might be used for tracer particles in the PIV analysis on the boundary were excessively eliminated. Therefore, an appropriate decision of threshold level was needed to resolve these problems, and the value fit for aim was chosen to be 20 % higher than the background -subtracted level, to give some tolerance in setting the base level. The selected threshold level was enough to remove unwanted background noises and to include drifting small droplets around the spray. Because the background intensity levels were rather low on the whole, a bit "generous" decision of threshold (120 % of background-subtracted level) was acceptable.

3. Entropy Analysis

The fundamental theory for entropy analysis using laser scattering image is based on the statistical thermodynamic entropy concept, which is a result of Boltzmann's work upon the relation between probability and entropy. A few studies for turbulent gas jets have already been published using this concept with slight modifications (Yuyama et al., 2000; Kando et al., 1999). Entropy represents not only the spatial regularity, but also reflects the state of disorder as defined by the original concept. So it can be said the entropy concept substantially expresses the real mixing state with physical meaning, and this is its merit over the other definitions.

W is the number of a case for groups that consist of particles of N_i, whose energy levels ($E_i=\varepsilon_i N_i$, ε_i=specific energy of group N_i) are different, to be distinguished from each other.

In a laser scattering image, if the number of particle in each interrogation area divided by M is expressed as N_i, W can be defined as products of combinations of N_i like as follows:-

$$W={}_N C_{N_1}\times{}_{(N-N_1)}C_{N_2}\times\cdots\times{}_{N_M}C_{N_M}=\frac{N!}{N_1!N_2!N_3!\cdots N_M!}=\frac{N!}{\prod N!} \quad (1)$$

where, N : is the total number of particles in the interrogation area M : Number of meshes

Entropy, according to Boltzmann's statistical concept, is defined as shown in Eq. (2), making the assumption that $N\gg 1$ and by substituting Eq. (1).

$$S=k\ln(W)=k[N\cdot\ln(N)-\sum_i\{N_i\cdot\ln(N_i)\}] \quad (2)$$

where, k : is Boltzmann's constant

N : total number of particles in the interrogation area

N_i : Number of particles in individual grid

By assuming that Ni is proportional to the intensity of each pixel, the entropy can be expressed as follows:-

$$S=\alpha\cdot\sum I_i\cdot\ln\{\alpha\cdot\sum I_i\}-\sum[\alpha\cdot I_i\cdot\ln(\alpha\cdot I_i)] \quad (3)$$

$$=\alpha\cdot\sum_i I_i\cdot\ln\{\sum_i I_i\}-\alpha\cdot\sum_i I_i\cdot\ln(I_i)$$

where, α : is a proportionality factor
I_i : the intensity of an individual pixel

Assuming the case of the homogeneous state, Eq. (3) can be described as Eq. (4) from the standpoint of mean value.

$$S=\alpha\cdot I_t\cdot\ln(I_t)-\alpha\cdot I_t\cdot\ln(I_t)/M \\ =\alpha\cdot I_t\cdot\ln(M) \quad (4)$$

where, I_t : is the sum of intensities in the total area.

M : Number of meshes

The value to represent the least entropy can be defined as shown in Eq. (5), making an assumption that the least case is calculated by subtracting the intensity values of highest degree (256 degree for 8-bit image) from other intensity data in the interrogation area when all the intensities are binarized to 0 and 255 (Yuyama et al., 2000).

$$S=\alpha\cdot[\ln(I_t)-A\cdot I_{max}\cdot\ln(I_{max})] \\ =\alpha\cdot[I_t\cdot\ln(I_t)-I_t\cdot\ln(I_{max})] \quad (5)$$

where, A : is the number of meshes on which the intensity levels are all at maximum

I_{max} : Maximum intensity level (for example, 255 for a 8 bit image) Finally, the normalized entropy expressing homogeneity is defined as follows.

$$\bar{S}=\frac{S-S_0}{S_1-S_0}=\frac{I_t\cdot\ln(I_{max})-\sum_i\{I_i\cdot\ln(I_i)\}}{I_t\cdot\{\ln(M)-\ln(I_t)+\ln(I_{max})\}} \quad (6)$$

where, S_0 : is the entropy in the initial state before mixing.

S_1 : is the entropy when all the particles are uniformly scattered in the space

In this work, entropy variations due to the ambient conditions were investigated by using the normalized entropy of Eq. (6). The normalized entropy has a maximum value of 1 and by its definition, tends to 1 if the particles are homogeneously distributed in all meshes.

However, this analyzing technique has some disadvantages. The entropy value calculated by this method is very sensitive to the choice of interrogation regions, mainly to the mesh size or the portion of scattered intensities relative to the background portion. Also it is impossible to distinguish the real homogeneous state formed by scattered particles from the homogeneous "black" background. In other words, some errors may occur in estimating the real state between the homogeneous black and the homogeneous white because homogeneous black may be also regarded as homogeneously diffused or distributed state. Thus, another effort was made to circumvent these shortcomings by adopting new concept that involves neighbor meshes (Yuyama et al., 2000). But, this concept was also not robust in terms of the selection of the interrogation region, and requires careful attention in use. So, in our work, the original concept was used without any modification rather than using an alternative.

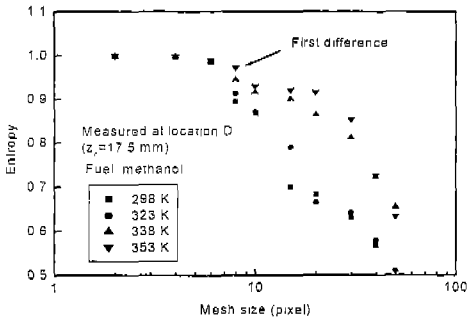

Fig. 4 Sensitiveness of entropy to the selection of mesh size

Figure 4 shows an example on the sensitiveness of entropy levels to the mesh sizes, measured at location D (z_c=17.5 mm) of methanol spray for different ambient temperature conditions. Entropy values change to the selection of mesh sizes. Those values are nearly constant up to the mesh size of 6 pixels, irrespective of ambient temperature conditions. But at the mesh size of 8 pixels, some differences are firstly seen. Those differences grow as the mesh sizes are increased, with particular fashions according to the ambient temperature conditions. This results means that if the mesh size is less than some critical value, no differences can be detectable because small spots less than mesh resolution may be regarded as homogeneous by themselves. To the contrary, the

entropy levels drop on increasing the mesh sizes because the larger mesh may contain more irregularities. So, a certain fixed proper mesh size should be determined to contain the equal levels of irregularities and the fixed mesh size of 8 pixels, at which the first differences were seen, was chosen for current study. Therefore, all the entropy values shown were calculated, after dividing the local interrogation area by the fixed mesh size of 8 pixels.

Another weak point of entropy analysis is that the entropy levels abruptly may change on the border line, such as the spray boundary. However, in current study, these drawbacks could be avoided by the careful choice of interrogation regions, meshes of proper sizes and a constant portion (70%) of scattered intensities that constitute an interrogation area relative to the background portion.

Therefore, our work could be progressed without adopting further newly created techniques.

4. Results and Discussion

The analyses of our results show, macroscopic changes of spray shape due to the change of ambient and fuel conditions. The calculation of entropy from scattering images, the distribution of velocity and vorticity calculated by PIV, the relation between entropy and vorticity, and effect of ambient composition are also presented.

4.1 Macroscopic behavior of the spray

To define the spray tip penetration and spray angle, all the images were binarized to clearly distinguish the spray periphery, after firstly removing weak intensity levels in terms of threshold value. Due to the macroscopic characteristics of the spray in our work, which means a near constant cone angle that persists to the spray tip, a measurement of spray angle was straightforward. But the determination of a standard to define spray tip penetration was quite difficult. So we defined the location of furthest droplets, as the spray tip penetration. For each experimental condition, values taken from 15 images were averaged for the calculation.

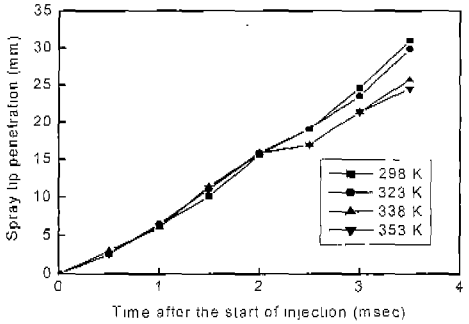

Fig. 5 Spray tip penetrations for the lapse of time and ambient temperature

Figure 5 shows the penetration of methanol spray to ambient temperature for the lapse of time. If 3.5 ms after the start of injection is regarded as a measuring point, the spray tip penetration decreases as ambient temperature increases because of vaporization. In particular at over 338 K, the vaporization effect downstream of the spray after 2.5 ms is noticeable.

Figures 6 and 7 show the spray tip penetrations and spray angles for methanol and M85 measured 3.5 ms after the start of the injection, respectively. Concerning the term for spray, and because spray angle is practically the same as cone angle under our experimental condition, spray angle is used without special classification. For the two fuels, spray tip penetrations decrease and, conversely, spray angles increase with increases of ambient temperature. With increased ambient temperature, the downstream part of the spray vaporizes and the radial dispersion improves because the fuel viscosity decreases and expansion due to decreased local fuel density is followed. The expansion in the axial direction due to vaporization could not be measured because the instant for image capturing was presumably after significant portion of spray downstream had vaporized.

The spray tip penetrations seem to be nearly equal for the two fuel sprays, but slight differences were seen for spray angles. A similar result was also shown in another study (Miko and Buoyan, 1992). That is probably because of the difference between the vaporization characteristics of the two fuels. In contrast with methanol, that has

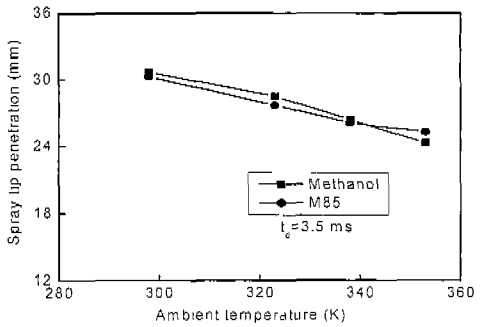

Fig. 6 Comparison of spray tip penetrations between methanol and M85 for ambient temperature

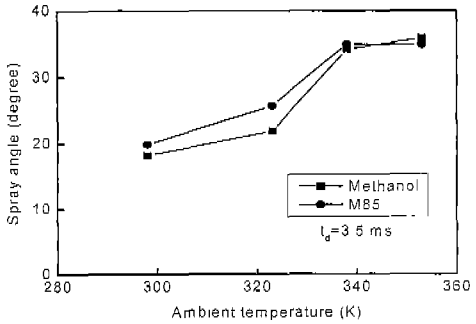

Fig. 7 Comparision of spray angles between methanol and M85 for ambient temperature

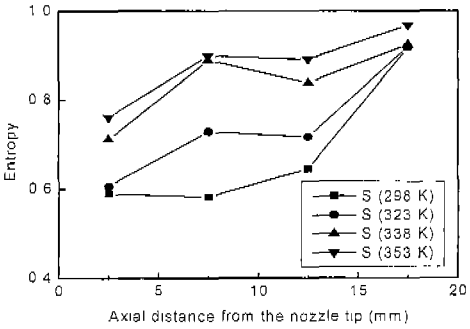

Fig. 8 Entropy variation for methanol

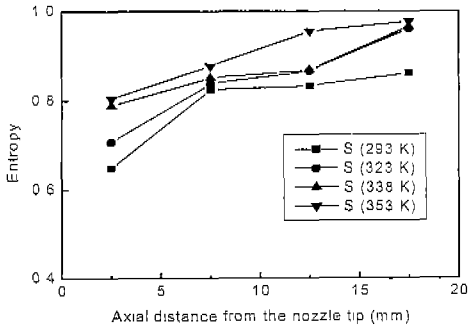

Fig. 9 Entropy variation for M85

single boiling point because it is a pure substance, M85 contains gasoline that has wide boiling point (300-443 K). So, even if the ambient temperature is below 338 K, some vaporization of M85 can occur, which promotes dispersion to the ambient and causes a slight increase in the spray angle. Changes in spray angle are more sensitive to vaporization than penetration dominantly driven by axial momentum. On the other hand, at temperatures above the boiling point of methanol (338 K), the vaporization rate of methanol exceeds than that of M85, which contains components of higher boiling points.

4.2 Entropy analysis

In this section, the effect of ambient temperature is shown on the entropy level according to distance from the nozzle exit.

In the non-vaporizing condition, even if there were some variations, the spray tip penetration and angle are almost constant when they are averaged. But, since all these features are changed abruptly as ambient temperature increases, it is impossible to describe the characteristics of each location by setting interrogation cells at fixed positions. Therefore, the position of each cell was determined to be variable, considering the change of the spray shape, to reflect the representative characteristics of each location.

The interrogation regions are placed on the relative positions in y-direction to the locations shown in reference image of Fig. 3. But, the positions in x-direction were chosen for the portion filled with scattered intensities, distinguished from background one in each interrogation area, to be 70 % after image processing to make clear the spray boundary. But the real portions including all the neighboring values around the main spray can be different case by case due to drifting droplets. Each interrogation region of 64×64 pixels included the boundaries between spray and ambient. The intensity data was extracted from scattering images by 256 degrees.

Figures 8 and 9 show the entropy variations for methanol and M85 sprays to the changes of location and ambient temperature. On going from A to D, say, to the downstream, entropy increases and becomes nearly constant at D. The entropy increases as the ambient temperature increases, showing an particularly abrupt change above the boiling point of methanol (323 K). Entropy values of M85 are higher than those of methanol on the whole and also show higher values below 323 K. It is thought that this is possibly due to the 'drifting fine droplets' scattered around the main spray, which are suspected to be gasoline. Since the entropy is regarded to increase if small droplets are homogeneously filled in the interrogation meshes, high values of entropy are obtained for M85 due to such scattered droplets. The effect may also be due to the vaporization of low boiling point components in the gasoline. The differences shown in the results are rather large considering the small difference in the compositions of the two fuels, say, only 15%. This result implies that the possibility that the M85 spray is well mixed may be high, even though the fact that the effective mixing or diffusion of spray to the ambient really occurs is not yet specifically confirmed.

The improvement of cold startability with M85 is predominantly due to the physical characteristics of fuel, but the fact that 'drifting fine droplets' formed around the main spray may help to form a mixture, which is also proven by the increased entropy. The reason why the entropy increases on moving downstream is possibly due to the increased entraining motion induced by viscous friction and dispersion after the end of injection. But under the vaporizing conditions, dilution due to the decreased density and random motions of vaporizing droplets are taken as major factors that contribute to the increase of entropy. So in the following sections, the effects of these factors on the mixing are investigated by correlating the velocity and vorticity distributions obtained by PIV with entropy.

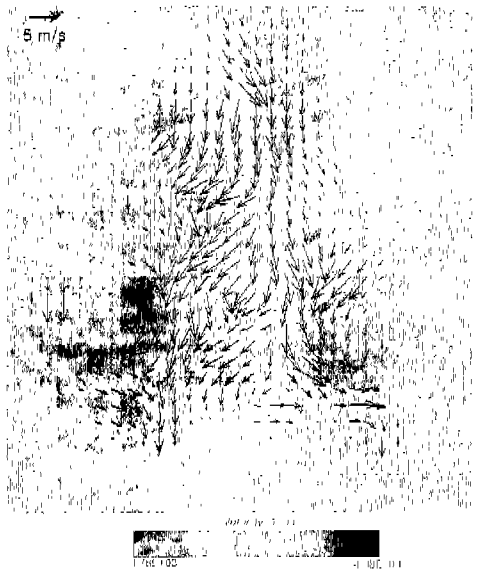

Fig. 10 An example of PIV image interrogated on whole spray for methanol at T_{amb}=323 K

4.3 PIV analysis

The PIV analysis was used to determine the fluid dynamic information, such as the velocity and vorticity distributions. Local interrogation regions were same as shown in Fig. 3.

Figure 10 is an example of a PIV analysis on entire spray scale of the methanol spray (T_{amb}= 338 K). Minimum interrogation grid size was set to 10×10 pixels for the whole spray scale analysis and 8×8 pixels for local region analysis.

On moving downstream, some regions where the radii of vorticities become large are observed, possible mixing with air may also occur. In particular the effect of vaporization on the velocity and of the vorticity fields at downstream of the spray is apparent.

4.4 Relation between vorticity strength and entropy

Increased entropy means improved mixedness. Assuming the factors that increase the entropy are: a) viscous friction induced by velocity gradient and b) vaporization, we investigated the relation between vorticity and entropy, as well as the effect of vaporization. Since vorticity represents the velocity gradient, here, vorticity strength is used as the means of expressing viscous friction

while neglecting viscosity variations. It is necessary to note here that the vorticity shown in our work represents the motion on a macro scale rather than on a micro scale, due to the limitations of image resolution. However, the entropy concept is based on the assumption of micro scale motion. Both values experience limitation in terms of resolution but the entropy value is less sensitive, by definition as applied in our work. Thus, taking our assumption to be valid, each value represents motion in a different scale.

The regions for entropy and vorticity analysis are same. Vorticity strength shown as a single value is normalized, expressing the absolute strength of vorticity, which is defined as shown in Eq. (7).

$$\bar{w}_z=\sum_i |\omega_{z,i}| / \sum\sum_i |\omega_{z,i}| \qquad (7)$$

That is, it is the sum of the absolute values of the vorticities on every minimum grid in each interrogation region, divided by total sum of absolute vorticities in four interrogation regions. In general, these values get larger on moving to downstream of the spray. However, this order is not always valid, and is often changed by ambient condition or measured time.

To clarify the relation between vorticity strength and entropy, the variation mode of vorticity strength to the change of axial location was beforehand examined. Figure 11 and 12 show the variation of vorticity strenth to the axial location for methanol and M85 spray, respectively. For both cases, the vorticity strengths appear to increase on moving to downstream of the spray. Particularly, the vorticity strengths get large with near-linear slope before the proportionalities slightly tend to decrease at location D (z_c=17.5 mm). From these results, it can be thought that the vorticity strength increases on moving to downstream of the spray, though this result may be affected by some experimental conditions, such as measured time, or ambient gas conditions. In our experimental condition, an image is captured when the injection is just ended. At that time, the spray becomes fully grown and the spray boundary shape is kept at near straight

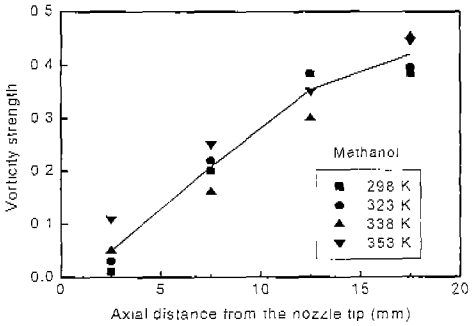

Fig. 11 Variation of vorticity strength for distance from the nozzle tip

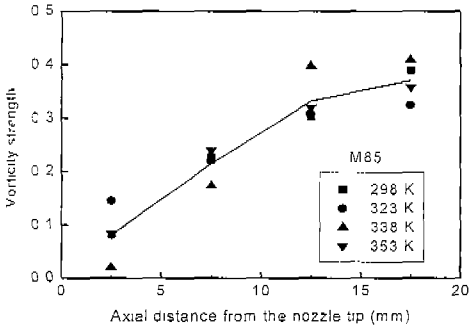

Fig. 12 Variation of vorticity strength for distance from the nozzle tip

line, which may be interpreted as velocity gradient persists, at least up to C (z_c=12.5 mm). Judging from the results of Figs. 11 and 12, it would be difficult to distinguish the difference of variation mode to the axial location for two fuel sprays. So an assumption that vorticity strength approximately can be used on behalf of the axial location may help to explain the further results in alternative manner, based on the close relationship between the two, as shown in Fig. 11 and 12.

Figure 13 shows the relation between vorticity strength and entropy and the ambient temperature conditions. The values of vorticity strengths used as an independence variable on abscissa resulted from Figs. 11 and 12. Classifying the ambient conditions as (a) T_{amb}=298~323 K and (b) T_{amb}=338~353 K, the difference in the changes phases can be easily detected. Before vaporization, the entropy increases in an exponential fashion. But at ambient conditions above the vaporization temperature, entropy is

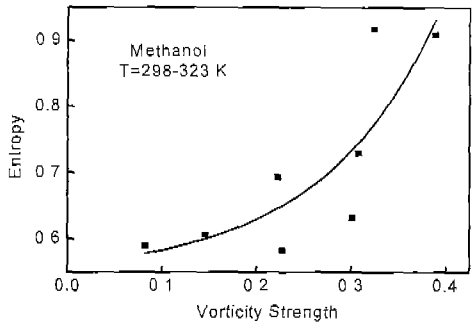

(a) T_{amb}=298-323 K

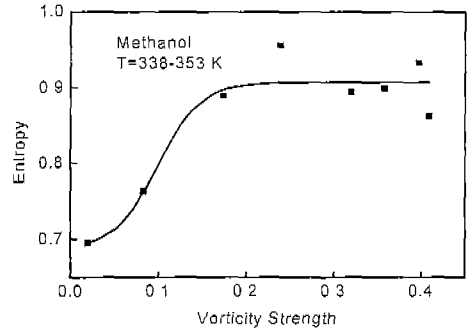

(b) T_{amb}=338-353 K

Fig. 13 Relation between vorticity and entropy for methanol spray

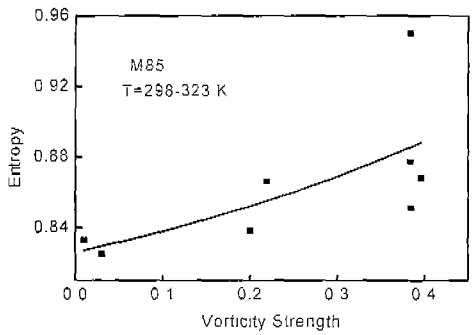

(a) T_{amb}=298-323 K

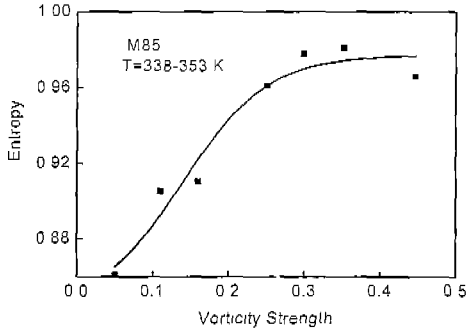

(b) T_{amb}=338-353 K

Fig. 14 Relation between vorticity and entropy for M85 spray

proportional to the vorticity strength only on the upstream part of spray, where the vorticity value is generally low, and after that entropy becomes nearly independent of vorticity. From these results, it is found that the velocity gradient induced by viscous friction does not affect the increase of entropy as the vaporization progresses, particularly in the lower part of spray.

Figure 14 is the relation between vorticity strength and entropy for the M85 spray. The trend seen is very similar to that shown in Fig. 13. For (a) T_{amb}=298~323 K, although the slope is rather gentle compared with that of the methanol spray, the entropy continuously increases with increased vorticity. For (b) T_{amb}=338~353 K, though the slope is somewhat steeper than that of the methanol spray, entropy increases for a certain value of vorticity strength and after that it becomes independent of vorticity, as shown in Fig. 13.

The reason why the degree of dependency is different can be inferred from the difference in the vaporization characteristics of the two fuels and the definition of entropy. It is thought that the gentle slope of proportionality for the methanol spray in (a) T_{amb}=298~323 K is probably due to part-vaporization of low boiling point components in M85, weakening viscous friction. For the rather high slope of proportionality in (b) T_{amb}=338~353 K, there is the effect of high boiling point components in gasoline. Whether these components really survive the effect of viscous friction in the vaporizing environment needs more detail investigation. Once again, as mentioned in Fig. 8 and Fig. 9, because of the ' drifting fine droplets' suspected as gasoline in spray, the entropy becomes somewhat higher than that of methanol.

4.5 Effect of ambient gas conditions

Figure 15 shows the effect of changing ambient conditions by the controlled addition of CO_2. The fuel tested is methanol at T_{amb}=323 K. The interrogation region of interest is C, as shown in

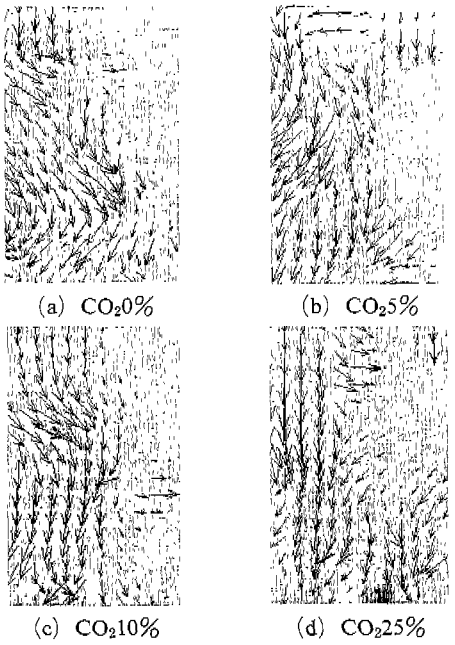

Fig. 15 Velocity and vorticity distributions for different ambient gas composition (location C shown in Fig. 3)

Fig. 3. But its size is increased in the y-direction (64×100 pixels).

CO_2 that is usually supplied by EGR, is one of the low viscosity gases likely to exist in the intake ports. Since the viscosity of CO_2 is lower than that of air by a factor of 1.9 (Adrian, 1994) under our experimental conditions, velocity and vorticity distributions can be changed accordingly compared with the normal case. In the case of zero CO_2 addition, the radial velocity components become stronger and the spray width becomes wider, especially in the lower part of the interrogation region.

The case of 5 % CO_2 is similar to that of 0 %, but stronger axial components on the spray boundary are seen when the CO_2 addition ratio increases from 10 to 25 %.

The result implies that the spray width (or the spray angle) decreases with increased CO_2 addition ratio. This is probably resulted from the difference in the viscosity of the ambient gas, but the effect of density variation induced by CO_2 addition also should be considered. If the ambient temperature and pressure are maintained to fixed

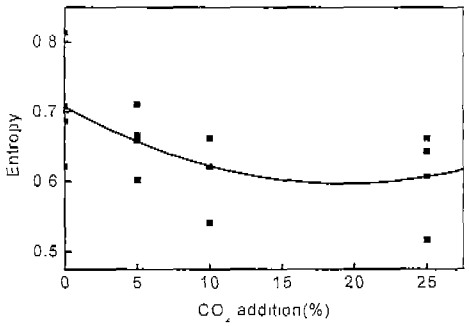

Fig. 16 Relation between ambient composition and entropy (location C shown in Fig. 3)

values, the density varies in proportion to molecular weight. So the addition of CO_2 leads to the increased ambient density, relative to that of normal air. In general, the spray width becomes narrower with decreased ambient density or viscosity, due to decreased aerodynamic or viscous drag. Here, CO_2 addition has the opposite effect on the spray shape in terms of viscosity and density, i. e. , one decreases and the other increases the spray angle. But based upon the result that the active radial spreading tendency is lower at lower CO_2 additions, it would appear that the viscous effect is more dominant, at least, under our experimental conditions. But quantitative comparisons of the relative strengths of these effects could not be made, because of the minor differences in physical properties in our narrow experimental range of interest.

Although, the degree of mixing can be inferred qualitatively from velocity and vorticity distributions, entropy analysis may be introduced once again to show the phase of changes for some other interrogation areas.

Figure 16 shows the variation of entropies versus the CO_2 addition ratio for the same conditions as shown in Fig. 15. Entropy values for regions B, C, and D were correlated. As the CO_2 ratio increases, these values seem to decrease despite some scatter, showing some hint of being insensitive to further gas composition variations. But considering only the current result, this result is possibly due to decreased ambient viscosity to lead the mixing. The influence of increased density, with an increase in the CO_2 addition ratio,

also can be considered as a factor that induces drag. But its effect is hidden by the 'slim shape of spray' (narrow spray cone angle) at higher CO_2 addition ratios, representing the viscous effect. Were this experiment done under high-pressure injection or high-pressure ambient condition, there would a more distinct difference in the entropies, due to an increase in ambient resistance and viscous friction.

5. Conclusions

Laser scattering images were used to investigate the characteristics of methanol and methanol blended sprays under non-vaporizing and vaporizing ambient conditions. With the aid of some parameters, several conclusions were obtained as follows.

(1) There are differences in the macroscopic behaviors or methanol and methanol blended sprays, with increased ambient temperature. The spray tip penetrations are nearly the same for the two sprays. However, the spray angle of the M85 spray is slightly greater than that of the methanol spray below the vaporization temperature of methanol, though at temperatures greater than this the spray angle of methanol becomes greater than that of M85.

(2) The entropy of the M85 spray is higher than that of the methanol spray on the whole. The entropy values of the methanol spray begin to increase rather drastically above the vaporization temperature of M85.

(3) There is some proportionality between the vorticity strength and entropy below the vaporization temperature of methanol. However, the proportional relation is no longer valid above the vaporization temperature, when the entropy becomes independent of vorticity strength.

(4) Under the same pressure and temperature conditions, the spray width and entropy tends to decrease with increasing levels of CO_2 in the ambient gas.

Acknowledgements

This research was supported by the International Cooperation Program of KISTEP (2000) and also funded by the R. A. Support Program of BK21 (2000)

References

Adrian Bejan, 1994, *Convection Heat Transfer*, John Wiley & Sons, Inc. , pp 603~604.

Kazuyoshi, N., Hiromi, N., Kakuro, K. and Daijiro, H., 1989, "Development of Ultrasonic Atomizer and its Application to S. I. Engines," *SAE* Paper 890430.

Kim, Y. K., Iwai, N., Suto, H. and Tsuraga, T., 1980, "Improvement of Alcohol Engine Performance by Flash Boiling Injection," *JSAE Review*, Vol. 2, pp. 81~86.

Kondo, T., Chikahisa, T. and Hishinuma, Y., 1999, "Turbulent Mixing for Effective Soot Reduction during Combustion Process," *The 15th Internal Combustion Engine Sympo.* (Int.).

Lee, N. H., Park, J. H. and Choi, K. H., 1999, "A Study on Fuel Spray of Spark-Ignited Direct Injection Engine Using Laser Image Technology," *KSME Int. Journal*, Vol. 13, No. 1.

Lee, S. H., Shin, Y. K. and Hwang, S. S., "Experimental Study on the Improvement of Cold Startability of Methanol (M85) Fueled Engine," *Journal of KSAE*, Vol. 14, No. 3.

Michael, Z. and Eran S., 1996, "Fuel Atomization by Flashing of a Volatile Liquid in a Liquid Jet," *SAE Paper 960111.*

Miko, F. and Buoyan Xu, 1992, "Spray Characteristics of Methanol-Gasoline Blends Using Ultrasonic Atomizer," SAE Paper 922353.

Suga, T., Kitajima, S., Kobayashi, Y., Nagashima, T., Sato, K. and Inudo, N., 1990, "Development of Methanol Vehicles," HONDA R&D Technical Review, Vol. 2, pp. 100~110.

Yuyama, R., Chikahisa, T. and Hishinuma, Y., 2000, "Microscopic Diffusion Phenomena and Air Entrainment into Turbulent Jets," *The 16th Internal Combustion Engine Sympo.* (Int.).